External forcing of Moon and Earth seismicity at Rieger periods

Mensur Omerbashich
https://orcid.org/0000-0003-1823-4721, editor@geophysicsjournal.com

Abstract: As I recently showed from InSight mission 2018-2020 data, seismicity on magnetically defenseless Mars arises in a planetary rupturing response to Rieger instability of the interplanetary magnetic field (IMF) in the 1–6-month (385.8–64.3-nHz) band of highest solar-system energies. I next examine lunar and terrestrial seismicity in the same bend. Moonquakes and earthquakes during traversals of the Earth magnetotail were analyzed separately from IMF events to decouple magnetosphere and IMF effects. The analysis showed with 99–67% confidence and very high (Φ>>12) fidelity that (an unspecified majority of) moonquakes and M_w5.6+ earthquakes also reoccur at Rieger periods. About half of the spectral peaks split but into clusters that average to the usual Rieger periodicities also, where magnetotail reconnecting clears the signal. This confirmation of the Mars result means that Rieger disturbance of the IMF co-drives dynamics of solid-surface bodies, including the Moon and, to an extent, magnetically shielded Earth.

Keywords—Moon seismicity; Earth seismicity; Mars seismicity; planetary physics; Rieger process.

---

1. Background and motivation

Omerbashich (2021a) recently showed that, in the absence of an inherent magnetic field and plate tectonics, seismicity on Mars is generated externally by Rieger resonant process. The P_{Rg} = 154-day *Rieger period* (Rieger et al., 1984) and its 5/6 P_{Rg}, 2/3 P_{Rg}, 1/2 P_{Rg}, 1/3 P_{Rg} , and 1/5 P_{Rg} harmonics, i.e., ~128, ~102, ~78, ~51, and ~31-days periods called Rieger-type periodicities (Dimitropoulou et al., 2008) characterize the Rieger process of instability. A damped, periodically forced nonlinear oscillator, which exhibits both periodic and chaotic behavior, successfully simulates this process (Bai and Cliver, 1990). Importantly, P_{Rg} resonance was detected in the interplanetary magnetic field (IMF), including IMF in the Earth's vicinity (Cane et al., 1998). Previously, Simpson (1968) posited that IMF variations could cause seismic rupture via a magnetohydrodynamic coupling or surging the crustal currents.

In addition to IMF, the peculiar Rieger process was reported from most types of heliophysics data in solar cycles 19–24, such as flares, photospheric magnetic flux, group sunspot numbers, and proton speed. In the past, Rieger periods have been reported in different ranges, depending on data, location, epoch, and methodology, as 155–160 days, 160–165 days, 175–188 days, and 180–190 days; see, e.g., Gurgenashvili et al. (2017). Most of those studies indicate a leading (longest) periodicity ranging from 152- to 158-days, which appears to be dominant particularly in the time phase from ~1979–1983, corresponding to the solar activity maximum. (Chowdhury et al., 2008) The same agents that force solar activity could be responsible for at least some geomagnetic and seismic activity (Odintsov et al., 2006), as found to be the case for Mars (Omerbashich, 2021a).

Demonstration of the criticality of the Rieger process for Mars planetary dynamics warrants further investigation. Then in what follows, I use all available data for our solar system — namely time-series of seismic events occurrences on Earth and Moon — in an integrative approach to examine the role of the Rieger process in generating seismicity on other solid-surface bodies besides Mars.

2. Data and methods

For the above purpose, I look into the 1–6-months spectral band, representing the solar system's overall most energetic dynamics, as the band in which the Rieger process controls marsquakes (Omerbashich, 2021a). The Rieger process involves the heliosphere proper, IMF, and possibly other solid-surface bodies in addition to Mars.

2.1 Moon data

The moonquake data consisted of 13058 seismic events from the 1981 *Levent.1008* Moonquakes Catalog (Nakamura et al., 1981) (updated in 2008), sampled at the 17-mHz rate (once per minute) from 1969-1977 by the Apollo Program's passive seismic experiment—ALSEA (missions 11–16). Previously, Omerbashich (2020b) had used those data in their raw form to demonstrate the superharmonic resonance mechanism for generating lunar seismicity. Here I use the same data but remove meteoroid, rocket, Lunar Module impacts, and events with duplicate sampling time-stamps to enable time-series monotony. The removal resulted in a dataset of 10815 genuine natural moonquakes, Appendix A, plotted on Fig. 1 indiscriminately for a most realistic depiction of any driving processes. Since there still exists no consistent definition of moonquake magnitude (Nakamura, 2019), the lunar events were assigned generic random magnitudes (Omerbashich, 2020a).

2.2 Earth data

The data represented the Earth's strong seismicity sampled at 1Hz rate, in moment magnitudes *Mw* as the most realistic (physics-based) representation of seismicity (Kanamori, 1977) (Dziewonski & al., 1981). The data set consisted of occurrence times of all q = 866 earthquakes of M_w5.6+ to within 10^{-1}, spanning Δt = 1211 days from 01 October 2015–02 February 2019; see Appendix B. The robust (outliers M^{**} discarded) means from the USGS, EMSC, and GFZ moment magnitudes were spectrally analyzed, as:

$$\overline{M_i}|_{i=1}^{q} = \frac{1}{3}[M_i^{USGS} + M_i^{EMSC} + M_i^{GFZ}];\ \ i \in \aleph\ \wedge\ \overline{M_i}|_{i=1}^{q} \Leftrightarrow M_i \neq M^{**}, \tag{1}$$

Here, I tacitly assume that any excess events close in time and space to the event strongest for such time clusters would overrepresent the seismic response to the Rieger process rather than enrich its depiction. Hence to prepare data, I decluster the record to eliminate redundancy, thus excluding the 21 events that had occurred within minutes of time and location of another, so that I kept the strongest events per time cluster if any. This declustering resulted in 845 occurrences of M_w5.6+ events. Previously, Omerbashich (2020a) used the same data to demonstrate the superharmonic resonance mechanism for generating Earth seismicity.

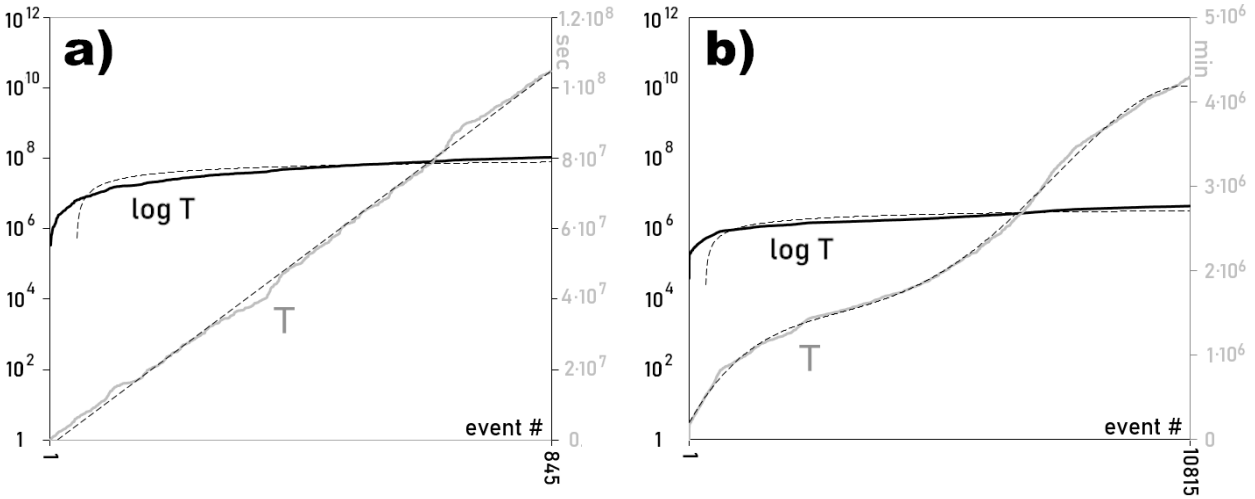

Figure 1. Occurrences, T, of 845 consecutive M_w5.6+ strong earthquakes from 2015–2019 (panel **a**) and 10815 consecutive natural moonquakes from 1969-1977, i.e., excluding meteoroid, rocket, and Lunar Module impacts, as well as events with duplicate sampling timestamp (**b**), plotted indiscriminately for a more natural depiction of driving processes. Time-series data commonly are plotted along manmade equipaced-time axes, which, as such, largely mask any nonlinear background dynamics. Both panels: solid gray line represents T in seconds of Earth time (panel **a**) and minutes (**b**); the solid black line is the plot of *log*T. Also plotted are respective trends (gray dashed): linear — revealing a nonlinear background process as it attempts to drive terrestrial seismicity but gets suppressed (panel **a**), and the 4th order polynomial trend — revealing a free nonlinear background process as it intensely forces lunar seismicity periodically in that process's own (unspecified) timeframe (**b**). Superimposed ideal logarithmic trends (black dashed) highlights temporal inflection points of the process. Note that the shown processes and trends depend on neither the event source nor rupturing size, indicating an externally induced seismicity, more so in the Moon case. Assuming IMF variations commonly generate seismicity on solid-surface bodies, the revealed trends mean the Rieger process affects Moon immensely and Earth to an extent. Event-times reduced to 0-origin. See Appendices for data sets.

2.3 Data separation

Due to the inherent instability of magnetism, and under the assumption that the Rieger-forced seismicity is not Mars-specific, we cannot expect the Rieger process to be reflected in magnetospheres and respective local IMF simultaneously. Thus, when a planetary magnetosphere oscillates with a certain Rieger period, the IMF in that planet's vicinity does not necessarily match that period exactly (or it oscillates with another Rieger period altogether), and vice versa.

Harada et al. (2010) showed a magnetic effect of the Earth's magnetotail on the Moon, using data from the 2007-2009 SELENE (Kaguya) lunar mission to demonstrate a strong electric field near the lunar surface during Moon traversing the magnetotail where plasma conditions are significantly different from those in the IMF. This relatively intense and mutable electric field arises when otherwise magnetism-stripped Moon passes through the plasma sheet residing centrally in the magnetotail.

To examine the effects of the Earth magnetotail on terrestrial and lunar seismicity, I take advantage of GVSA blindness to data gaps and separate natural moonquakes into segments when the Moon was inside the Earth magnetotail (2865 events), i.e., within three days of the Full Moon (Phillips, 2008), v. IMF (7950 events), i.e., the rest of the data set. The separation of earthquake data has resulted in time series with 210 and 635 events, respectively. Indeed, this procedure exposes the above mismatch of zonal periodicity, Figure 2. As seen, the Earth magnetotail is responsible for most of the mismatch between the lunar seismic response and the Rieger process tacitly assumed representable by a polynomial trend, thus exposing the process as inherent to the IMF, as expected.

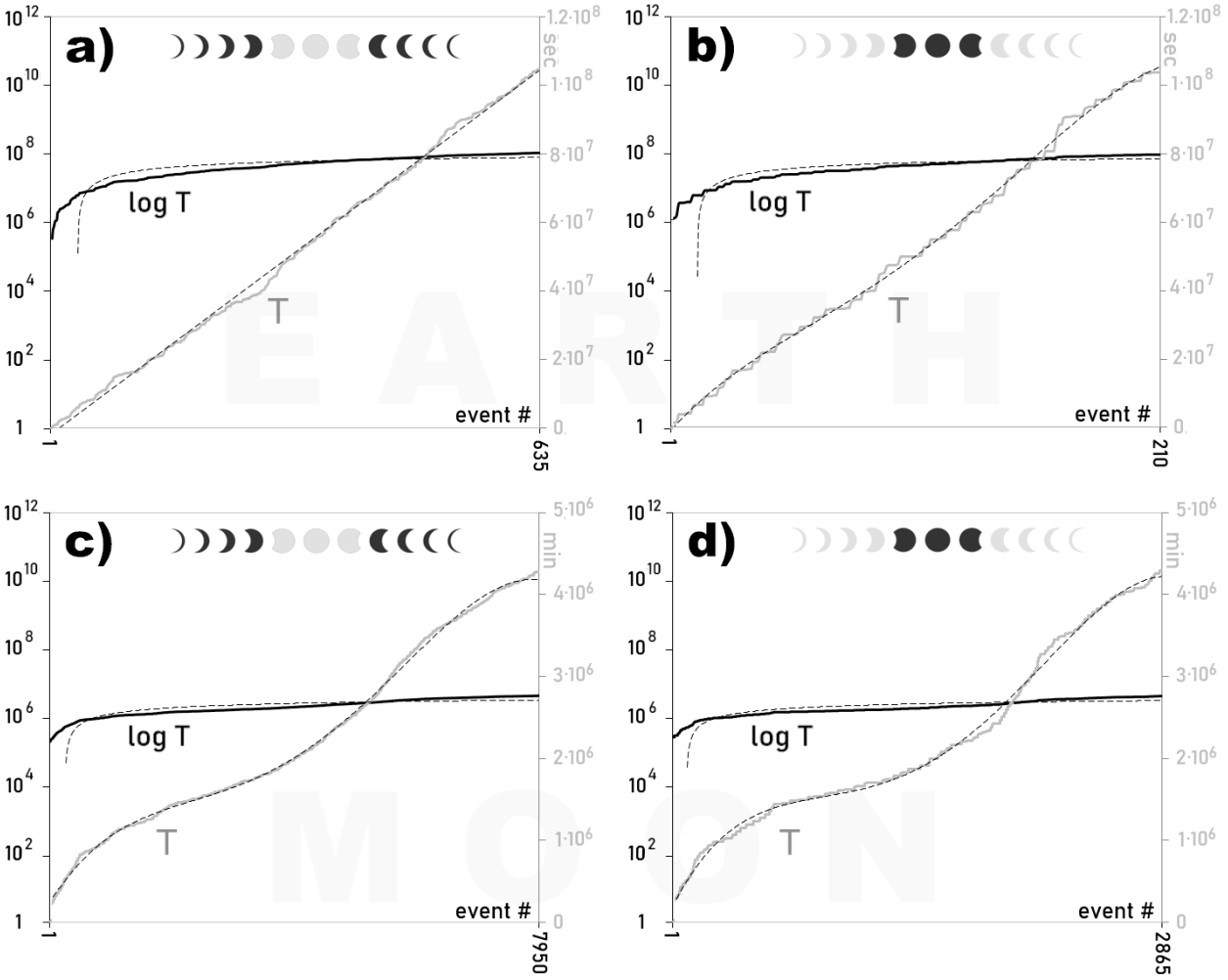

Figure 2. Indiscriminately plotted M_w5.6+ strong terrestrial (top row) and lunar (bottom) events occurrences, T, from Fig. 1, separated into events during the Moon's traversals of the Earth's magnetotail (panels b & d), v. during traversing the IMF (panels a & c). As in Fig.1, a nonlinear background driver of strong terrestrial seismicity is seen as suppressed (panel a) but then resumes nonlinearity (as fitted weakly by the 4th order polynomial) as the Moon crosses the Earth's magnetotail. This switch from suppressed to free nonlinearity of terrestrial seismicity occurrences as the Moon moves from the IMF to magnetotail reveals that the Moon's opposition disturbs a dynamic of the Earth-Moon system (bodies magnetism reconnecting). This dynamic then is seismogenic itself. Furthermore, the nonlinearity of the dominant forcing process of terrestrial seismicity is weaker than the nonlinearity of the lunar seismicity's forcing process, so different nonlinear dynamics dominate the two bodies. A distinctively better match of moonquakes occurrences to the 4th order polynomial in panel c v. panel d reveals that the lunar seismicity occurrences are nonlinear most faithfully while the Moon traverses the IMF and that the magnetotail affects the nonlinearity. This causality, in turn, indicates that the main driver of lunar seismicity lies in the IMF as this seismicity arises magnetohydrodynamically, with the Moon's response to IMF variability boosted on each reconnection with the Earth magnetotail. Note that here one magnetotail traversal begins three days before a lunar opposition (Full Moon) and lasts for six days (Phillips, 2008), so Moon spends about 25% of its orbital travel inside the Earth's magnetotail. Lines representation is as in Fig. 1. See Appendices for data sets.

2.4 Methodology

To analyze the seismicity occurrences, I apply the Gauss–Vaníček rigorous method of spectral analysis (GVSA) by Vaníček (1969, 1971) for computing spectra by a least-squares fit of data periodicity and trigonometric functions. The GV spectra were computed with k = 1000 spectral resolution throughout, as:

$$s_j^{GVSA}\left(T_j, M_j^{GVSA}\right);\ j = 1 \ldots k \ \wedge \ k \in \aleph\,. \tag{2}$$

GVSA has numerous advantages over the Fourier class of spectral analysis techniques in analyzing sparse natural data of long spans (Press et al., 2007; Taylor, 1972). The method provides absolute extraction accuracy in analyzing even the extremely (over 99%) gapped records of data (Omerbashich, 2006, 2007a). Subsequently, the method went through simplifications — into non-rigorous (strictly non-least-squares) formats, such as the Lomb-Scargle technique. GVSA provides total accuracy in extracting periods from natural data sets — to the prescribed accuracy of analyzed data themselves (Omerbashich, 2021b). Once fed raw data, the GVSA outputs spectra with spectral magnitudes in variance percentages, var%, or decibels, dB (Pagiatakis, 1999) against linear background noise levels. The method enables relative spectral computations whose results for physical systems are directly energy-stratified, enabling direct separation of resonance forcers from respective harmonics and other systematic signal contents. Here, input data are used in their raw form, i.e., without preprocessing (such as 0-padding, filtering, decimating, windowing, and tapering) or post-processing used by some to enhance spectra. Declared precision on detected spectral peaks is ±1'.

3. Results and discussion

The process responsible for IMF disturbance at Rieger periods primarily reflects the flapping of solar wind, plasma, and other types of mechanical waves (composed of electrons mostly) as they get pushed outwards by coronal mass ejections. As with any mechanical resonance, which arises as waves incur insurmountable obstacles, the Rieger periods themselves are naturally occurring resonance harmonics of the electromagnetic blanket's dynamics as the IMF experiences different influences exerted by the solar system's bodies and their dynamics and gravitation.

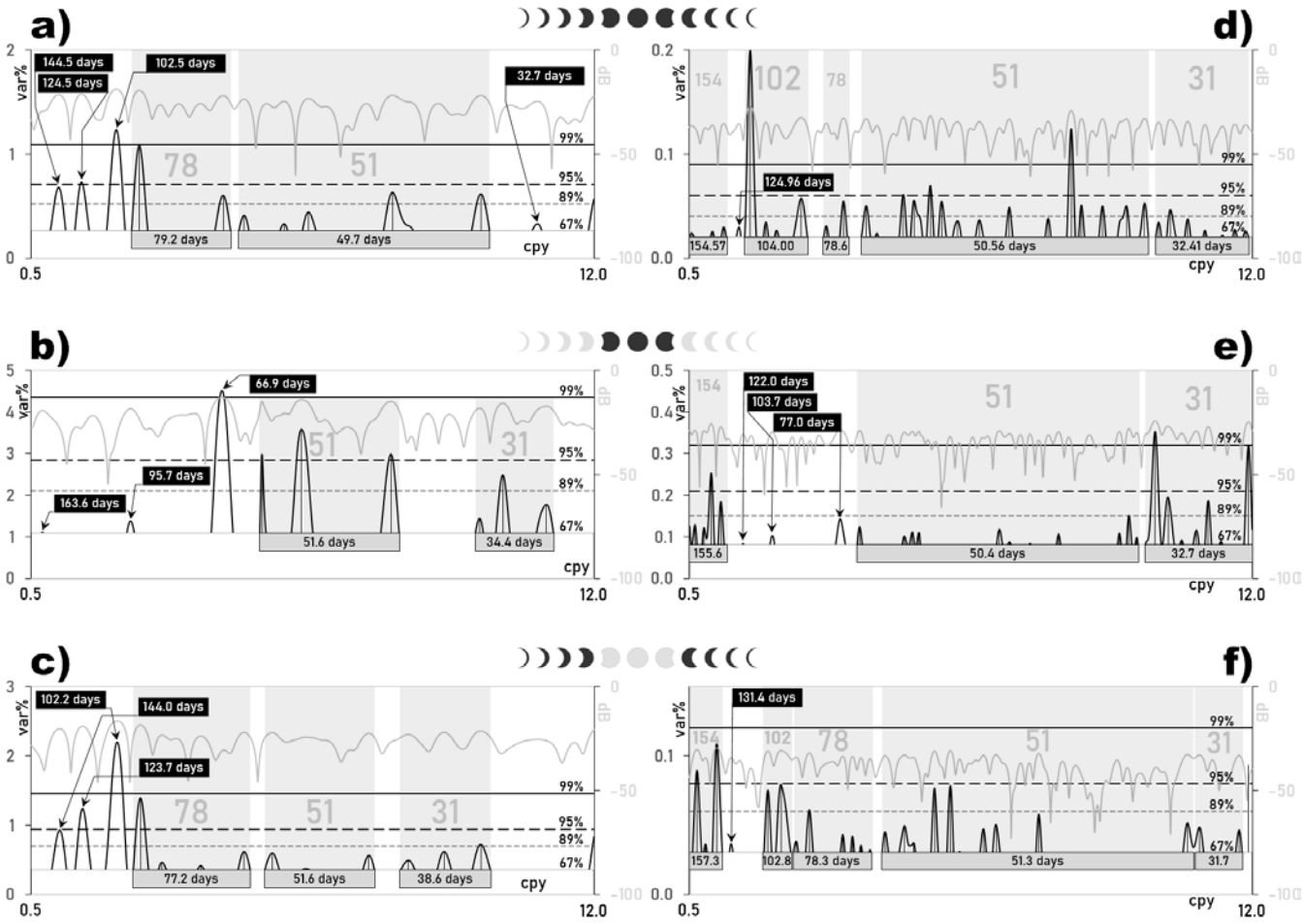

Figure 3. Significant peaks of GV variance spectra (dark line), in var%, and power spectra (gray), in dB — of terrestrial (left column) and lunar (right) seismicity occurrences, Figs 1&2 and Appendices A&B. Shown are all events (top row), events while the Moon was traversing Earth's magnetotail (middle), and events while the Moon was traversing IMF (bottom). Events in all cases respond with all Rieger periods, except during the Moon's traversals of the magnetotail resulting in suppressing of the 128-days primary harmonic in terrestrial seismicity (panel b). Despite splitting into clusters (gray boxes) within relatively powerless spectral subbands (gray lobes getting narrower or less pronounced), all the clusters average to Rieger periods as well, Table 1. Statistical fidelity for the above spectra is very high (Φ>>12), ranging from low to high frequencies as $7.5 \cdot 10^6$–$3.8 \cdot 10^4$ and $7.5 \cdot 10^3$–$2.2 \cdot 10^2$ for terrestrial and lunar seismicity, respectively. Rieger periods reported most often are 154-, 128-, 102-, 78-, 51-, and 31-days, but, depending on data type/epoch and processing methodology, the periods were reported in other ranges as well; see, e.g., Gurgenashvili et al. (2017).

3.1 Moon

Celestial bodies sample the IMF-resident Rieger process rotationally — as seen in the example of Mars (Omerbashich, 2021a). Thus, while traveling along its orbit around the Earth, the magnetism-stripped Moon samples both the Earth's magnetotail region (for ~1/3 of a revolution or synchronous rotation) and IMF (~2/3). As a result of constant mutual interference by the smaller and magnetism-stripped Moon against the more massive and magnetically shielded Earth, half of Rieger periods in earthquakes occurrences and 5 of 6 periods in moonquakes occurrences split while the Moon traverses IMF, Fig. 3 — but into clusters that in all cases average to Rieger periods as well.

Furthermore, the Moon's connecting with the Earth's magnetosphere lowers the interference significantly (clears the signal), bringing the number of split spectral peaks in the Earth's seismic response to the Rieger process down from 3 to 2, Fig. 4-b v. Fig. 4-c, and in the Moon's response from 5 to 3, Fig.

4-e v. Fig. 4-f. Note that spectral magnitudes in lunar seismicity spectra are here again as in (Omerbashich 2020a, 2020b) an order of magnitude smaller than in terrestrial seismicity spectra, as expected because moonquakes are far weaker than earthquakes. This energy-proportionate response reflects on the power spectra also, as narrower and less pronounced gray lobes, see left v. right columns of Fig. 3. Also, note that a significance at or above 67% suffices for confirmation of widely reported physical period ensembles, as is the case here.

The non-stratified lunar seismicity shows no clear orbital preference; thus, moonquakes had occurred significantly more often neither when the Moon was in the Earth magnetotail nor the IMF. The interference of Rieger resonance waves by the magnetotail has boosted the power both band-wide (widened or otherwise more pronounced lobes in power spectra) and in GVSA-typical depictions of field energy levels against the linear variance background (Omerbashich, 2007b), seen here as spectral peaks doubling in magnitudes, middle row of Fig. 3.

The differences in spectral frequencies of the Moon v. Earth seismic response to the IMF-residing Rieger process, Table 2, measures the mismatch of individual Rieger periodicities due to different dynamics affecting the ecliptic's blanket of solar ejecta and wind. This mismatch can serve as a gauge for determining the wavelengths of Rieger resonance dynamically and map its change with time.

The main reason why previous spectral analyses of earthquakes and moonquakes occurrences returned no Rieger periodicities is in using either all or stratified data; e.g., Bulow et al. (2007) examined time series of deep moonquakes. Namely, when all events are analyzed combined, the resulting spectra contain the Rieger process, albeit masked behind a combined magnetotail and magnetosphere interference, so that moonquakes return clustered periods only, Fig. 3-d. In earthquakes, such spectra cluster for most of the band, and the lowest Rieger frequencies get significantly mismatched due to other geodynamical drivers sharing the high-energies bands.

	P_i within tail [days]	P_i within IMF [days]	$P_i^{average}$ [days]	P_i^{common} [days]	Δ [days]	Δ [%]
Earth	163.6	144	153.8	154	0.2	0.1%
Moon	155.6	157.3	156.4	154	-2.4	-1.6%
Earth	x	123.7c	123.7	128	4.3	3.4%
Moon	122	131.4	126.7	128	1.3	1.0%
Earth	95.7	102.2	99	102	3	2.9%
Moon	103.7	102.8c	103.2	102	-1.2	-1.2%
Earth	66.9	77.2c	72.1	78	5.9	7.6%
Moon	77	78.3c	77.6	78	0.4	0.5%
Earth	51.6c	51.6c	51.6	51	-0.6	-1.2%
Moon	50.4c	51.3c	50.9	51	0.1	0.2%
Earth	34.4	38.6	36.5	31	-5.5	-17.7%
Moon	32.7	31.7	32.2	31	-1.2	-3.9%

Table 2. The matching of Rieger periods as estimated from the spectra of earthquakes and moonquakes occurrences, Fig. 3 and Table 1, and the most commonly reported respective values. The averaged Rieger period, PRg, is closer to the most often-reported value for Earth than for Moon. All averaged Rieger-type periodicities (resonance harmonics) agree better with the respective commonly reported values for Moon than for Earth. This comprehensive inconsistency indicates that different processes dominate seismicity on the two bodies. When the Moon was in the Earth magnetotail, interference suppressed the 128-days (primary harmonic), allowing the power to shift to other periods whose peak magnitudes then doubled, revealing that Moon influence on earthquakes is primarily magnetic and alternating. This suppression of a long Rieger period (the strongest harmonic) in the Earth seismic response to the Rieger process during magnetotail-Moon reconnections indicates that the Earth enjoys only slightly better protection from magnetically caused seismicity than the Moon does, as the Earth magnetosphere provides weak shielding so that even the Moon's trace magnetism can shut down the most energetic harmonic. On the other hand, the magnetism-stripped Moon responds to the entire Rieger process yieldingly.

T [days]	T_{Rg} [days]	T'_{Rg} [days]	ΔT [days]	ΔT [%]
From 845 (total) earthquakes:				
144.5498	144.5	154	9.45	6.1%
124.5291	124.5	128	3.47	2.7%
102.5200	102.5	102	-0.52	-0.5%
91.7917				
66.6247	79.2	78	-1.21	-1.5%
62.2430				
55.4316				
51.9861				
42.7735				
36.0433	49.7	51	1.30	2.6%
32.7303	32.7	31	-1.73	-5.6%
From 210 magnetotail earthquakes:				
163.6215	163.6	154	-9.62	-6.2%
95.6998	95.7	102	6.30	6.2%
66.8724	66.9	78	11.13	14.3%
58.9767				
52.9038				
42.9267	51.6	51	-0.60	-1.2%
36.1157				
34.6875				
32.2895	34.4	31	-3.36	-10.9%
From 635 IMF earthquakes:				
143.9712	144.0	154	10.03	6.5%
123.6726	123.7	128	4.33	3.4%
102.2285	102.2	102	-0.23	-0.2%
91.3255				
83.2886				
71.8131				
62.2430	77.2	78	0.83	1.1%
57.2858				
52.3646				
45.0225	51.6	51	-0.56	-1.1%
41.3474				
38.5549				
36.0433	38.6	31	-7.65	-24.7%

T [days]	T_{Rg} [days]	T'_{Rg} [days]	ΔT [days]	ΔT [%]
From 10815 (total) natural moonquakes:				
176.4671				
149.3522				
137.8988	154.6	154	-0.57	-0.4%
124.9618	125.0	128	3.04	2.4%
116.8421				
107.0995				
101.6507				
90.4072	104.0	102	-2.00	-2.0%
81.2195				
76.0660	78.6	78	-0.64	-0.8%
69.9961				
67.5000				
62.1355				
60.1606				
57.3772				
55.5171				
53.2169				
50.3839				
46.8403				
42.9780				
40.9706				
40.1474				
38.5549				
36.8937				
35.6857	50.6	51	0.44	0.9%
34.8218				
34.1279				
33.1832				
32.2605				
31.3877				
30.7964				
30.3033	32.4	31	-1.41	-4.6%
From 2865 magnetotail natural moonquakes:				
171.4204				
159.2737				
151.2363				
140.5942	155.6	154	-1.63	-1.1%
121.9946	122.0	128	6.01	4.7%
103.7024	103.7	102	-1.70	-1.7%
77.0437	77.0	78	0.96	1.2%
71.6700				
64.9404				
61.9215				
60.4640				
59.2683				
47.9648				
46.8403				
45.7092				
44.6869				
42.0730				
37.3536				
36.7055				
36.1884	50.4	51	0.55	1.1%
35.0253				
34.2906				
33.4923				
32.7005				
32.0878				
31.4701				
30.1762	32.7	31	-1.75	-5.6%
From 7950 IMF natural moonquakes:				
169.0038				
157.8753				
145.1332	157.3	154	-3.34	-2.2%
131.3514	131.4	128	-3.35	-2.6%
106.1511				
99.4030	102.8	102	-0.78	-0.8%
92.5000				
87.1221				
76.2272				
73.5761				
71.3855				
69.1881	78.3	78	-0.33	-0.4%
65.7718				
61.8151				
60.1606				
56.6541				
54.2607				
52.9817				
49.8254				
48.3517				
43.8692				
37.5094				
33.1832	51.3	51	-0.31	-0.6%
32.5525				
31.8886				
30.5868	31.7	31	-0.68	-2.2%

Table 1. Values for the GVSA spectra, Figure 3.

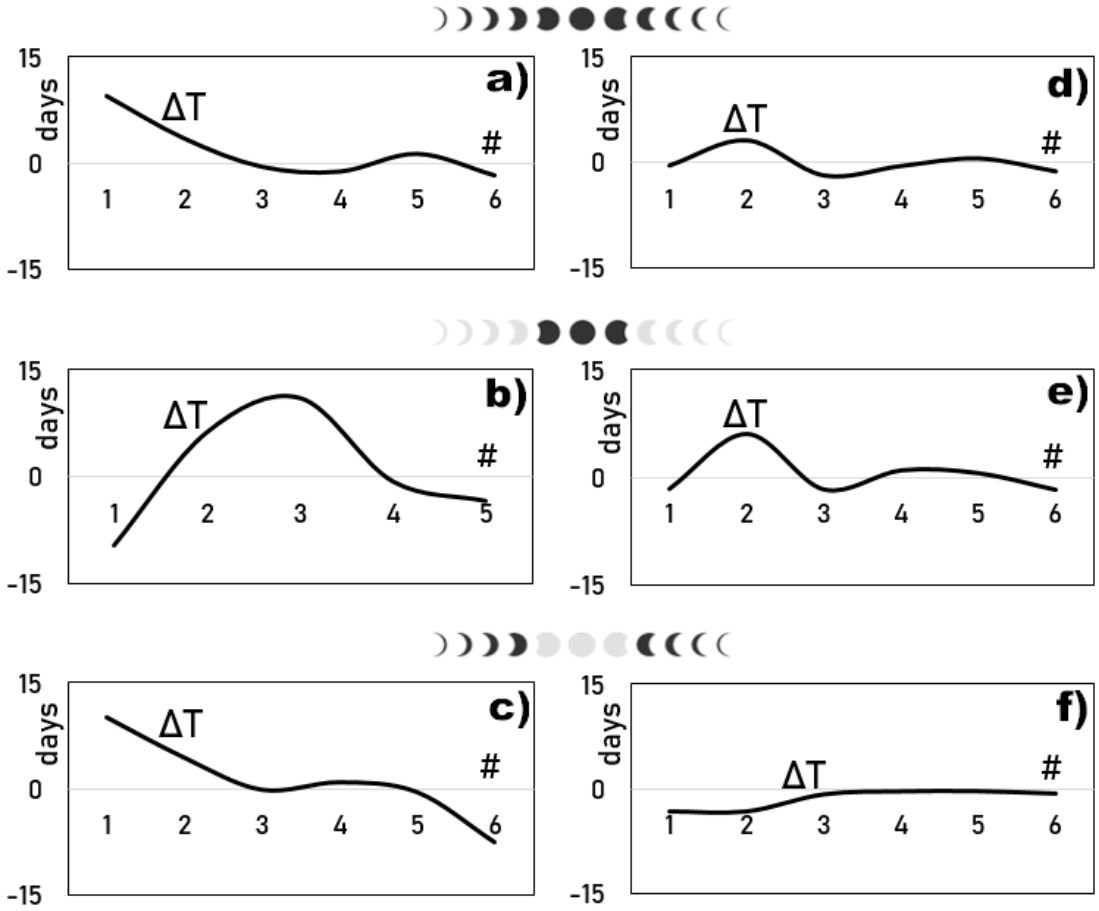

Figure 4. Matchings, ΔT, of most commonly reported Rieger periodicities to significant spectral peaks of earthquakes (left column) and moonquakes (right) occurrences, Figure 3, as the differences between all GVSA-estimated significant periods, Table 1, and the most commonly reported values of the nearest (first six) Rieger periods, respectively: ~154, ~128, ~102, ~78, ~51, ~31-days. Moon passages through the magnetotail cause the change in sign of the low-end mismatch as obtained from the terrestrial seismic response (to the Rieger process), panel b v. panel c. Similarly, the Earth magnetotail also interferes with the lunar seismic response in lower frequencies, panel e v. panel f. Finally, the matchings for magnetism-stripped Moon as it freely traverses the IMF are virtually absolute across the spectral band, panel f, revealing that the IMF affects lunar seismicity more than the Earth magnetosphere does.

3.2 Earth

The M_w5.6+ earthquakes occurrences reveal the Rieger period and weak and significantly offset periods from the Rieger, primarily and consistently in the low-frequency (most energetic) subband of the 1–6-month band. This apparent better sensitivity of earthquakes to the Rieger process in higher frequencies is expected not only because the Earth is magnetically shielded but also because the lunar orbit (T_{Moon} and $1/2T_{Moon}$) coincide with the $1/5P_{Rg}$ and $1/10P_{Rg}$ resonant harmonics, respectively — so that the tidal resonance of Earth demonstrated by Omerbashich (2020a) comes combined with the IMF's and Moon's magnetic influences.

Thus, the geodynamical impact of the Rieger process can be understood as coincidental since stronger, primarily gravitational-tidal, processes act upon Earth resonantly (*ibid*.) and at frequencies that are at the same time modifications of Rieger periods. On the other hand, the Earth magnetosphere generally is insufficient to filter out cosmic radiation, so the Rieger process could, in principle, constantly be injecting some energy that subsequently gets resonantly magnified and thereby contributes a significant force of geodynamics down to lower parts of the atmosphere. Then this excess irregular variation of electrons in the Earth atmosphere is likely due to Rieger forcing of the Earth and contributes to observed variations in the total electron content (TEC). Under this scenario, the magnetic shielding's inherent instability helps explain why the TEC precursory qualities are associated with earthquakes only rarely and irregularly, i.e., coincidentally so.

3.3 Discussion

As with any mechanical resonance that usually arises and can even get magnified due to obstacles in its propagation paths and other reasons, the above results suggest that the Rieger process itself is a state of continuous mechanical resonance of the solar ejecta within the solar wind blanketing the ecliptic. The process then occurs as the radiation in the solar system, with the Sun as the largest emitter, encounters obstacles — mainly in the form of rocky planets and moons, as well as occasional co-inclined visitor bodies like comets that remain confined close to the ecliptic for months or longer.

A generally held view is that moonquakes arise primarily due to the day-night thermal expansion of rock. However, sunlight too tenuously electrifies and ionizes the Moon (Halekas et al., 2018), so that a continuous magnetohydrodynamic interplay (of a weak electromagnetic field with trapped water molecules) could also be rupturing lunar rock — instead of or in combination with the thermal seismogenesis. The continuity of the interplay is supported further by a recent find that the Earth's magnetotail does not provide constant shielding to the Moon from outside particles (Shang et al., 2020).

Furthermore, modeling suggests that lunar hydrogen gets cumulatively depleted while Moon traverses the Earth magnetotail (Tucker et al., 2021). However, the hydration part of the interplay is supported further by the recent Chandrayaan-1 mission results showing that the Earth replenishes the lunar water supply via Earth magnetotail particles during each traversal — when a particle bridge gets established between the Earth and its natural satellite (Wang et al., 2021). Thus, the Earth's magnetosphere does possess the ability needed to reconnect with the Moon's magnetism regardless of the weakness and instability of the latter.

Finally, the Moon's ionosphere extends when shielded by Earth, resulting in the lunar plasma measurably perturbing the plasma coming from the Sun and the Earth and leading to observable changes in electrical currents and even the spatial distribution of electrons (Halekas et al., 2018).

Then the electromagnetic induction of lunar seismicity, as demonstrated in the present study, is similar to the mechanism for inducing seismicity on Mars (Omerbashich, 2021). However, the surging crustal currents and magnetohydrodynamic coupling mechanisms for an external generation of seismicity could be affecting the two bodies simultaneously but to a significantly different degree individually.

4. Conclusions

The Rieger process of resonant dynamics of the Sun's particle ejecta and the solar wind is reported commonly in most heliophysics data. As shown here and in the preceding areophysical study, the high-energies spectra of seismicity occurrences on all solid-surface bodies in the solar system for which data are available (Moon, Earth, Mars) are significantly periodic with Rieger periodicities only.

This find of an external and principal causal mechanism of natural seismic events warrants reinterpretation of the seismicity phenomenon to include the physics of a body-wide rupturing response of solid matter to variations in the interplanetary and other magnetic fields. In addition, the here presented results probably can be extended to apply to at least some of the Mw5.5- terrestrial seismicity as well.

Acknowledgments

I thank Dr. Ralph Lorenz (Johns Hopkins University) and Dr. Yosio Nakamura (University of Texas at Austin) for discussions and suggestions and to Barbara Pope (NASA-NSSDCA) for help with data. The least-squares spectral analysis scientific software LSSA, based on the rigorous method by Vaníček (1969, 1971), was used to compute spectra. Dr. Spiros Pagiatakis (York University) provided LSSA v.5.0, now available from http://www2.unb.ca/gge/Research/GRL/LSSA/sourceCode.html.

Data availability

The data underlying this article are available in the enclosed Appendices A and B.

References

Bai T. and Cliver E. W. (1990) A 154 day periodicity in the occurrence rate of proton flares. *Astrophys. J.* 363:299-309. DOI: https://doi.org/10.1086/169342

Bulow, R.C., Johnson, C.L., Bills, B.G., Shearer, P.M. (2007) Temporal and spatial properties of some deep moonquake clusters. *J. Geophys. Res.* 112:E09003. DOI: https://doi.org/10.1029/2006JE002847

Cane, H.V., Richardson, I.G., von Rosenvinge, T.T. (1998) Interplanetary magnetic field periodicity of ~153 days. *Geophys. Res. Lett.* 25(24):4437-4440. DOI: https://doi.org/10.1029/1998GL900208

Chowdhury, P., Kudela, K. Moon, YJ. (2016) A Study of Heliospheric Modulation and Periodicities of Galactic Cosmic Rays During Cycle 24. *Sol. Phys.* 291:581–602. DOI: https://doi.org/10.1007/s11207-015-0832-7

Dimitropoulou, M., Moussas, X., & Strintzi, D. (2008) Enhanced Rieger type periodicities' detection in X-ray solar flares and statistical validation of Rossby waves' existence. *Proc. Int. Astron. Union* 4(S257):159-163. DOI: https://doi.org/10.1017/S1743921309029226

Dziewonski, A.M., Chou, T.-A., Woodhouse, J.H. (1981) Determination of earthquake source parameters from waveform data for studies of global and regional seismicity. *J. Geophys. Res. - Solid Earth* 86(B4):2825-2852. DOI: https://doi.org/10.1029/JB086iB04p02825

Gurgenashvili, E., Zaqarashvili, T.V., Kukhianidze, V., Oliver, R., Ballester, J.L., Dikpati, M., McIntosh, S.W. (2017) North–South Asymmetry in Rieger-type Periodicity during Solar Cycles 19–23. *Astrophys. J.* 845(2):137-148. DOI: https://dx.doi.org/10.3847/1538-4357/aa830a

Harada, Y., Machida, S., Saito, Y., Yokota, S., Asamura, K. et al. (2010) Interaction between terrestrial plasma sheet electrons and the lunar surface: SELENE (Kaguya) observations, *Geophys. Res. Lett.* 37:L19202. DOI: https://doi.org/10.1029/2010GL044574

Halekas, J.S., Poppe, A.R., Harada, Y., Bonnell, J.W., Ergun, R.E., McFadden, J.P. (2018) A tenuous lunar ionosphere in the geomagnetic tail. *Geophys. Res. Lett.* 45:9450–9459. DOI: https://doi.org/10.1029/2018GL079936

Kanamori, H. (1977) The energy release in great earthquakes. *J. Geophys. Res. - Solid Earth Planets* 82(29):2981-2987. DOI: https://doi.org/10.1029/JB082i020p02981

Lou, Y.-Q., Wang, Y.-M., Fan, Z., Wang, S., Wang, J.X. (2003) Periodicities in solar coronal mass ejections. Monthly Notices of the Royal Astronomical Society 345(3):809–818. DOI: https://doi.org/10.1046/j.1365-8711.2003.06993.x

Nakamura, Y., (2019) Professor Emeritus of Selenophysics, University of Texas at Austin. *Personal Communication*, 27–28 March.

Nakamura, Y., Latham, G.V., Dorman, H.J., Harris, J.E. (1981) *Passive Seismic Experiment, Long Period Event Catalog, Final Version*. Institute for Geophysics, University of Texas at Austin. URI: https://hdl.handle.net/2152/65671

Odintsov, S., Boyarchuk, K., Georgieva, K., Kirov, B., Atanasov, D. (2006) Long-period trends in global seismic and geomagnetic activity and their relation to solar activity. *Phys. Chem. Earth* 31(1–3):88-93. DOI: https://doi.org/10.1016/j.pce.2005.03.004

Omerbashich, M. (2021b) Non-marine tetrapod extinctions solve extinction periodicity mystery. *Hist. Biol.* 34 (29 March). DOI: https://doi.org/10.1080/08912963.2021.1907367

Omerbashich, M. (2021a) Extramartian forcing of Mars seismicity at Rieger periods. *In review*. DOI: https://doi.org/10.5281/zenodo.4921735

Omerbashich, M. (2020b) Earth body resonance. *J. Geophys.* 63:15–29. ARK: https://n2t.net/ark:/88439/x020219

Omerbashich, M. (2020a) Moon body resonance. *J. Geophys.* 63:30–42. ARK: https://n2t.net/ark:/88439/x034508

Omerbashich M. (2007b) Magnification of mantle resonance as a cause of tectonics. *Geod. Acta.* 20(6):369–383. DOI: https://doi.org/10.3166/ga.20.369-383

Omerbashich, M. (2007a) Erratum due to journal error. *Comp. Sci. Eng.* 9(4):5–6. DOI: https://doi.org/10.1109/MCSE.2007.79; full text: https://arxiv.org/abs/math-ph/0608014

Omerbashich, M. (2006) Gauss–Vaníček Spectral Analysis of the Sepkoski Compendium: No New Life Cycles. *Comp. Sci. Eng.* 8(4):26–30. DOI: https://doi.org/10.1109/MCSE.2006.68

Pagiatakis, S. (1999) Stochastic significance of peaks in the least-squares spectrum. *J. Geod.* 73:67-78. DOI: https://doi.org/10.1007/s001900050220

Phillips, T. (2008) The Moon and the Magnetotail. NASA's Goddard Space Flight Center, NASA Space News, 16 Apr. http://web.archive.org/web/20210225013348/https://www.nasa.gov/topics/moonmars/features/magnetotail_080416.html

Press, W.H., Teukolsky, S.A., Vetterling, W.T., Flannery, B.P. (2007) *Numerical Recipes: The Art of Scientific Computing* (3rd Ed.). Cambridge University Press, United Kingdom. ISBN 9780521880688

Rieger, E., Share, G.H., Forrest, D.J., Kanbach, G., Reppin, C., Chupp, E.L. (1984) A 154-day periodicity in the occurrence of hard solar flares? *Nature* 312:623–625. DOI: https://doi.org/10.1038/312623a0

Shang, W.S., Tang, B.B., Shi, Q.Q., Tian, A.M., Zhou, X.-Y., Yao, Z.H., et al. (2020) Unusual location of the geotail magnetopause near lunar orbit: A case study. J. Geophys. Res. Space Phys. 125:e2019JA027401. DOI: https://doi.org/10.1029/2019JA027401

Simpson, J.F. (1968) Solar activity as a triggering mechanism for earthquakes. *Earth Planet. Sci. Lett.* 3:417-425. DOI: https://doi.org/10.1016/0012-821X(67)90071-4

Stallard, T.S., Baines, K.H., Melin, H., Bradley, T.J., Moore, L., O'Donoghue, J., Miller, S., Chowdhury, M.N., Badman, S.V., Allison, H.J., Roussos, E. (2019) Local-time averaged maps of H3+ emission, temperature and ion winds. Phil. Trans. R. Soc. A.3772018040520180405. DOI: https://doi.org/10.1098/rsta.2018.0405

Taylor, J., Hamilton, S. (1972) Some tests of the Vaníček Method of spectral analysis. *Astrophys. Space Sci.* 17:357–367. DOI: https://doi.org/10.1007/BF00642907

Tucker, O.J., Farrell, W.M., Poppe, A.R. (2021) On the effect of magnetospheric shielding on the lunar hydrogen cycle. J. Geophys. Res. Planets 126:e2020JE006552. DOI: https://doi.org/10.1029/2020JE006552

Vaníček, P. (1969) Approximate Spectral Analysis by Least-Squares Fit. *Astrophys. Space Sci.* 4(4):387–391. DOI: https://doi.org/10.1007/BF00651344

Vaníček, P. (1971) Further Development and Properties of the Spectral Analysis by Least-Squares Fit. *Astrophys. Space Sci.* 12(1):10–33. DOI: https://doi.org/10.1007/BF00656134

Wang, H.Z., Zhang, J., Shi, Q.Q., Saito, Y., Degeling, A.W., Rae, I.J., Zong, Q.G., Wei, Y., Liu, J., Guo, R.L. (2021) Earth Wind as a Possible Exogenous Source of Lunar Surface Hydration. Astrophys. J. Lett. 907(2):L32. DOI: https://doi.org/10.3847/2041-8213/abd559